Magnetic nanofluid properties as the heat transfer enhancement agent

Aleksandra Roszko[1,a] and Elzbieta Fornalik-Wajs[1]

[1]*AGH University of Science and Technology, Department of Fundamental Research in Energy Engineering, 30 Mickiewicz Ave., 30-059 Krakow, Poland*

Abstract. The main purpose of this paper was to investigate an influence of various parameters on the heat transfer processes with strong magnetic field utilization. Two positions of experimental enclosure in magnetic environment, two methods of preparation and three different concentrations of nanoparticles (0.0112, 0.056 and 0.112 vol.%) were taken into account together with the magnetic field strength. Analysed nanofluids consisted of distilled water (diamagnetic) and Cu/CuO particles (paramagnetic) of 40-60 nm size. The nanofluids components had different magnetic properties what caused complex interaction of forces' system. The heat transfer data and fluid flow structure demonstrated the influence of magnetic field on the convective phenomena. The most visible consequence of magnetic field application was the heat transfer enhancement and flow reorganization under applied conditions.

1 Introduction

Regarding the forthcoming thermo-ecological requirements there are a lot of issues devoted to improvement of existing technologies, increasing the efficiencies, emissions reduction, looking for a new devices and systems. In industrial applications increasing efficiency is very often identify with higher heat rate and flux transfer. Therefore one of the investigated ways to achieve it is connected with new fluids and their properties. Nanofluids become one of the analyzed options. The reason of their popularity comes from the properties and possible applications, e.g. heating of the buildings, solar absorption, energy storage, industrial cooling, friction reduction, nanodrug delivery, transportation, heat transfer intensification, etc [1]. Their properties differ from the common fluids, therefore they can replace them in existing processes or be used in new areas. There are many research devoted to the heat transfer processes intensification [2]–[5]. The first report on nanofluid successful preparation was in 1995 [6]. Since then, interest in such fluids is constantly growing.

Going toward the higher heat fluxes transfer the nanofluids appeared as the promising working fluids due to changes in the base fluid physical properties. Authors' goal was to check if the magnetic field can enhance heat transfer by low concentration nanofluids. The thesis that the nanofluid properties are the main parameters features and taking part in these processes was verified.

In this paper the experimental analysis of heat transfer and flow structure of diamagnetic, low concentration Cu/CuO nanofluids under the strong magnetic field are presented. Two positions of experimental enclosure in magnetic environment, two methods of preparation and three different concentrations of nanoparticles (0.0112, 0.056 and 0.112 vol.%) were taken into account together with the magnetic field strength. The fluctuations of temperature field were analyzed by Fast Fourier Transform and spectral analysis what led to the understanding of flow behavior under applied conditions. Through the results of mentioned analysis the magnetic field influence on the convective phenomena was valuated.

2 Experimental analysis

A schematic view of experimental set up and enclosure are presented in Figures 1 and 2. Experimental apparatus consisted of an cubical enclosure, a heater control system, a thermostating bath and a data acquisition system connected to a personal computer. A heating element was located under the bottom copper wall and was constructed with a nichrome wire. It was connected to a power supply monitored with the multimeters.

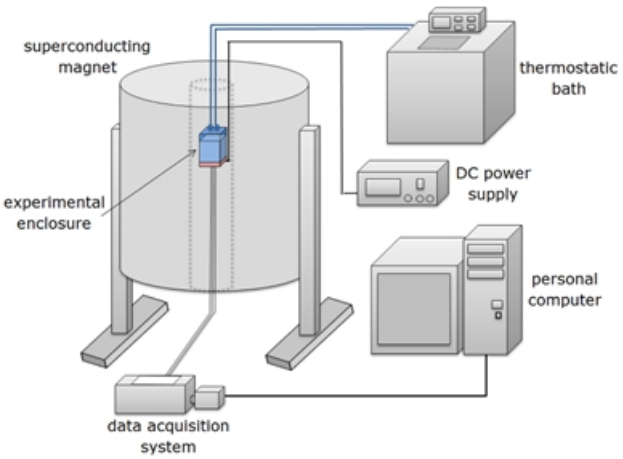

Figure 1. Schematic view of an experimental system.

[a] Corresponding author: roszko@agh.edu.pl

The cooling chamber being a part of enclosure was placed above the upper copper wall. Water flowing through the chamber assured the temperature maintained by the thermostating bath. The test vessel interior was a cube of 0.032 m size with heated bottom and cooled top horizontal walls. In one of the Plexiglas side walls six T-type thermocouples were placed to control temperature in the vicinity of that wall. The other six K-type thermocouples were located within the heated and cooled copper plates. The thermocouples' signals were recorded during whole experiment and enabled the post-processing analysis. The enclosure was filled with working fluid and positioned in the superconducting magnet test section. The cube locations were chosen for the sake of maximal value of magnetic induction square gradient ($\mathrm{grad}\mathbf{B}^2_{\max}$) occurrence, where magnitude of the magnetic force has the greatest influence. The working fluids were nanofluids with distilled water, as a base fluid, containing Cu/CuO nanoparticles of 40-60 nm diameter, prepared by two-step method. The properties of all examined fluids are presented in Table 1.

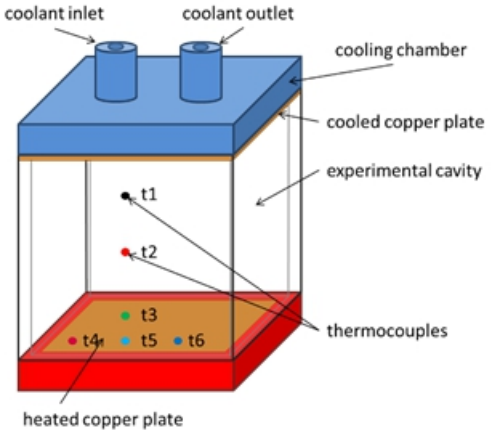

Figure 2. Experimental enclosure

The particular stages of experiment differed from each other in some details due to analysis of various parameters. However the main procedure remained the same. The heat transfer was evaluated through the Nusselt and thermo-magnetic Rayleigh numbers calculation. Definition of the Nusselt number applied in the studies took form:

$$\mathrm{Nu} = Q_{\mathrm{conv}} \cdot \left(Q_{\mathrm{cond}}\right)^{-1} \qquad (1)$$

where Q_{conv} is the convective heat rate and Q_{cond} is the conducted one. The thermo-magnetic Rayleigh number was define as follows:

$$\mathrm{Ra}_{\mathrm{TM}} = \mathrm{Ra}_{\mathrm{T}}\left[1 - \gamma B_z \left(B_{\max}\right)^{-1} \left(\partial B_z / \partial z\right)\left(B_{\max}\right)^{-1}\right], \quad (2)$$

where Ra_{T} is thermal Rayleigh number $\mathrm{Ra}_{\mathrm{T}} = g\beta\rho^2 c_{\mathrm{p}} \left(\mu k\right)^{-1} d^3 \Delta T$; g is the gravitational acceleration; β is the thermal expansion coefficient; ρ is the density; c_{p} is the specific heat; μ is the dynamic viscosity; k is the thermal conductivity; d is the characteristic dimension; ΔT is the temperature difference. The magnetization parameter γ was described by equation:

$$\gamma = \chi_m B^2_{\max} \left(\mu_m g d\right)^{-1} \qquad (3)$$

where: χ_m is the mass magnetic susceptibility; $B_{\max}$ is the magnetic induction in the centre of coil; B_z is the magnetic induction in the position of enclosure centre; μ_m is the vacuum magnetic permeability.

The first stage of whole measurement procedure was to determine heat losses dependence on temperature difference. It was assumed in the basis of [7] and verified experimentally that heat losses did not depend on phenomena occurring in the enclosure. Therefore, the formulas obtained in this stage were applied in all analysed cases. The heat losses were determined during the conduction state, which was established in the experimental cube turned upside-down (heated wall was at the top, while cooled one at the bottom). After stabilization of fluid and temperature stratification the measurements for various temperature differences were done. Detailed information and calculation scheme were presented in [8]. Following equations were obtained:

$$Q_{\mathrm{loss\_Cu0.0112}} = 0.0621 \cdot \Delta T \qquad (4)$$

$$Q_{\mathrm{loss\_Cu0.056}} = 0.0636 \cdot \Delta T \qquad (5)$$

$$Q_{\mathrm{loss\_Cu0.112}} = 0.0640 \cdot \Delta T \qquad (6)$$

The next stage of experimental procedure was connected with Rayleigh-Benard convection and magnetic influence on it. The temperature difference was set when magnetic field was off. Temperature of cooled wall was maintained at 18°C, what was equal to ambient temperature inside the magnet test section. Temperature of heated bottom wall depended on supplied heater power. The temperature difference was kept constant during the experiment. Therefore when heat transfer processes in the enclosure were changing

Table 1. Thermo-physical properties of all working nanofluids (at 293 K), * values measured

Property	Symbol	Unit	Cu0.0112		Cu0.056	Cu0.112
Thermal conductivity	k_{nf}	[W·(mK)$^{-1}$]	0.59862		0.59942	0.60042
Density	ρ_{nf}	[kg·m^{-3}]	999		1003	1007
Specific heat	c_{pnf}	[J·(kg·K)$^{-1}$]	4181		4180	4177
Thermal expans. coef.	β_{nf}	[K^{-1}]	$20.58 \cdot 10^{-5}$		$20.57 \cdot 10^{-5}$	$20.56 \cdot 10^{-5}$
Dynamic viscosity	μ_{nf}	[kg·(m·s)$^{-1}$]	$100.39 \cdot 10^{-5}$		$100.28 \cdot 10^{-5}$	$100.14 \cdot 10^{-5}$
Electrical conductivity	σ_{nf}	[S·m^{-1}]	$5.502 \cdot 10^{-6}$		$5.509 \cdot 10^{-6}$	$5.518 \cdot 10^{-6}$
Mass magn. susceptibility	χ_m	[m^3·kg^{-1}]	$-14.5 \cdot 10^{-9}$*	$-13.4 \cdot 10^{-9}$*	$-12.4 \cdot 10^{-9}$*	$-12.4 \cdot 10^{-9}$*
Nanofluids process mixing	-	-	mechanically	ultrasonically		

the supplied heater power was adjusted to obtain required temperature difference. After system stabilization the convection measurements were performed for the magnetic induction of 0, 2, 4, 6, 8 and 9T. When one step was completed the magnetic field induction was changed to next value and then it required about 1-2 hours to stabilize the system, once again.

The recorded thermocouples signals were a basis in the Fast Fourier Transform (FFT) and spectral analysis. These methods were chosen due to the nanofluids opaqueness and failure of optical ones.

To understand the influence of magnetic field on the convective phenomena occurring in the cubical enclosure the following parameters were studied: location of the enlosure in magnetic environment, the type of mixing (mechanical and ultrasonic agitation) and the nanoparticles concentration at various magnetic induction values.

3 Influence of maximal gradient location

This phase of experiment concerned position of the experimental enclosure in the magnet test section. The working fluid was nanofluid with distilled water, as a base fluid, containing Cu/CuO nanoparticles of 40-60 nm diameter, prepared by two-step method with mechanical mixing utilization for 8 hours. The resulting concentration of nanoparticles was 0.0112 vol.%. The temperature difference was about 3 K. The cube locations were chosen due to maximal value of gradient of magnetic induction square (grad$\mathbf{B}^2_{max}$) occurrence, where magnitude of the magnetic buoyancy force had the biggest influence. Theoretical considerations of forces acting in the systems led to that two locations of the cubical enclosure in magnet test section schematically shown in Figure 3. The scale of the arrows does not represent the real relation between the gravitational and magnetic buoyancy forces' magnitudes. They only indicated existed differences.

The forces acting on fluid in the system were defined as:

- the gravitational buoyancy force acting on diamagnetic fluid:
$$\mathbf{F}_g = -\mathbf{g}\rho\beta(T - T_0), \quad (7)$$
- the magnetic buoyancy force acting on diamagnetic fluid:
$$\mathbf{F}_m = -\chi_m \rho\beta(T - T_0)(2\mu_m)^{-1}\nabla\mathbf{B}^2_{max}, \quad (8)$$
- the magnetic force acting on paramagnetic particles:
$$\mathbf{f}_{m\_particle} = -\chi_m \rho(T - T_0)(T_0\, 2\mu_m)^{-1}\nabla\mathbf{B}^2_{max}, \quad (9)$$
- and the resultant force of the buoyant and gravity forces acting on paramagnetic particles:
$$\mathbf{F}_b = \rho_w \mathbf{g}V + \rho_{CuO}\mathbf{g}V \quad (10)$$

where: T_0 is the reference temperature equal to the arithmetical average of cooled and heated walls' temperature, χ is the volume magnetic susceptibility, V is the volume of particle.

In the position I the maximal value of grad$\mathbf{B}^2_{max}$ was situated in the middle of experimental enclosure and is represented as an ellipse in Figure 3. The magnetic

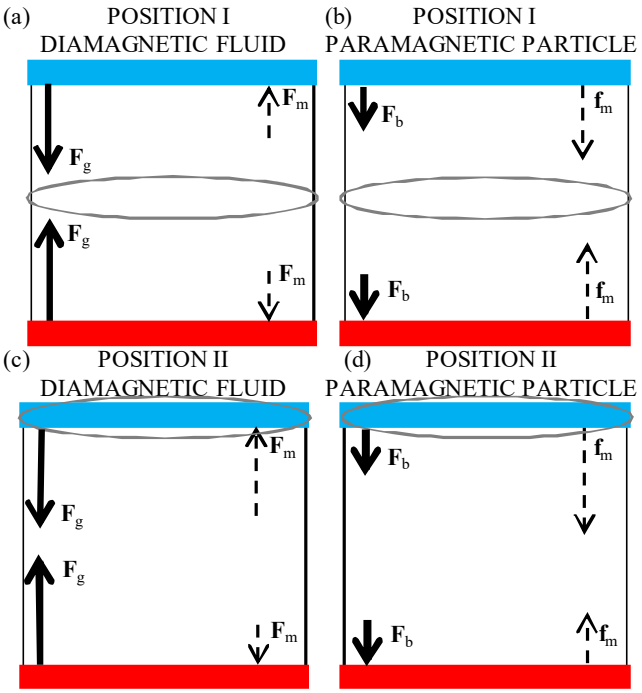

Figure 3. Schematic representation of the magnetic ($\mathbf{F}_m$) and gravitational ($\mathbf{F}_g$) buoyancy forces appearing in the system at position I acting on (a) diamagnetics, (b) paramagnetics and position II acting on (c) diamagnetics, (d) paramagnetics

and gravitational buoyancy forces acting on diamagnetics (water) are in opposite directions (Figure 3 (a)). The magnitudes of magnetization forces were similar due to the same distance between them and grad$\mathbf{B}^2_{max}$ position. Simultaneously, the magnetic buoyancy force acting on paramagnetic particles Cu/CuO were directed toward the maximum location (see Figure 3 (b)). The force magnitudes for paramagnetics were equal to each other but higher than for diamagnetics of about 10^3 times, however the particle concentration was low.

In the position II the maximal value of grad$\mathbf{B}^2_{max}$ was located on the upper (cooled) wall. Directions of acting forces were the same as in position I, although the magnitude of magnetic bouyancy forces acting in upper part of cube were greater than the ones in lower part of enclosure. It was caused by the distance from the maximal value of grad$\mathbf{B}^2_{max}$, the higher distance led to reduction of the magnetic buoyancy force value.

Summarizing the magnetic buoyancy forces acting on the diamagnetics caused convection attenuation while acting on the paramagnetics caused its enhancement. This complex reciprocal interaction of the forces came from the different magnetic properties of nanofluid components.

Dependence of the Nusselt number on thermo-magnetic Rayleigh number for two positions of the enclosure in the magnet test section is presented in Figure 4 (a). In both cases enhancement of heat transfer processes with increasing magnetic induction was of about 26% and about 13% in the first and the second enclosure positions, respectively. The theoretical considerations concerning the system of forces in both positions indicated that the attenuation of convection should be observed due to magnetic properties of water (which is diamagnetic).

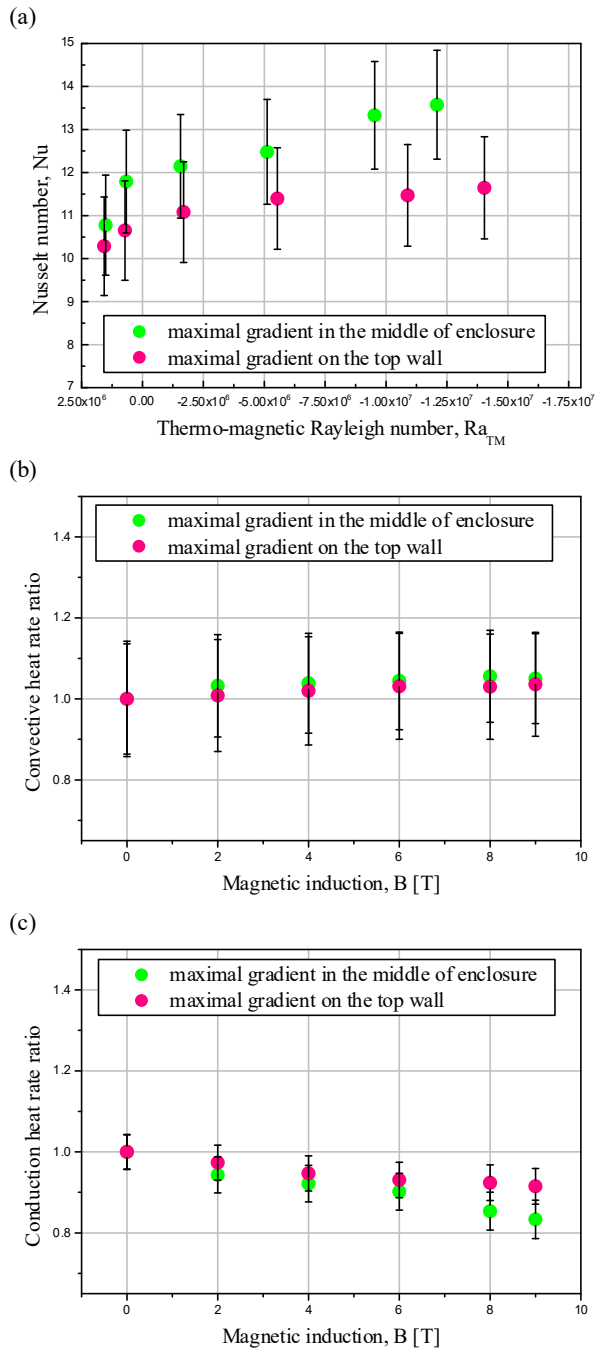

Figure 4. Heat transfer characteristics for various position of experimental enclosure in the magnetic field (a) The Nusselt number versus thermo-magnetic Rayleigh number; (b) convective and (c) conduction heat rate ratios versus magnetic induction

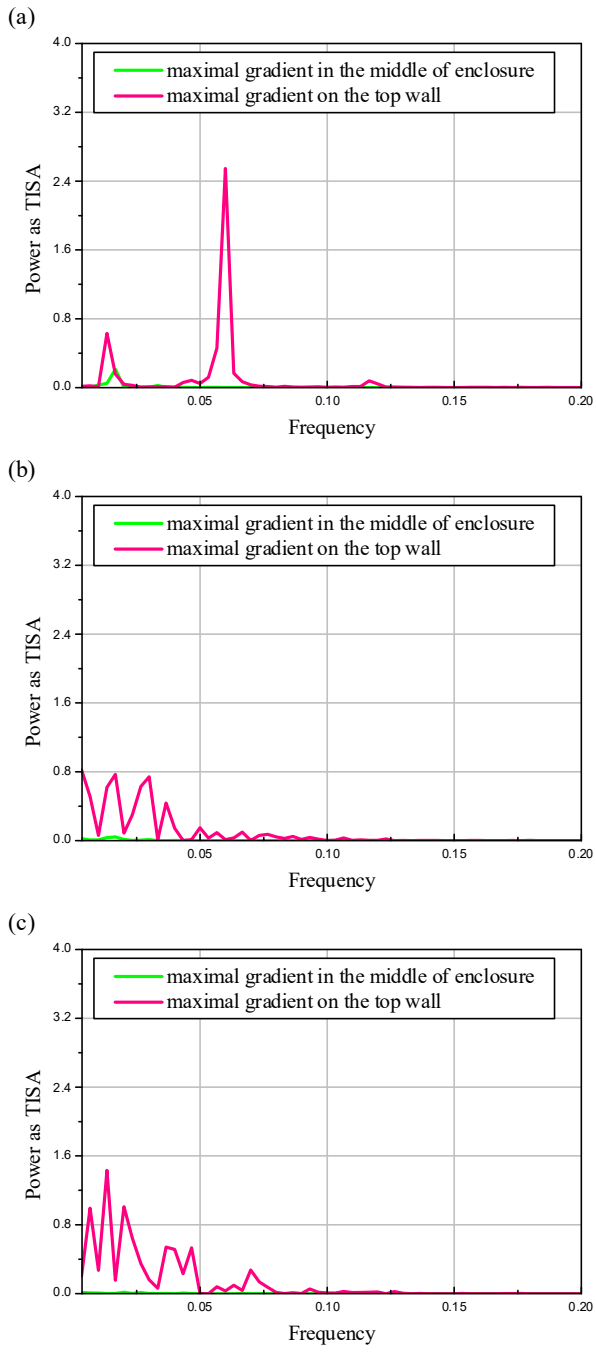

Figure 5. The power spectrum versus frequency for t6 thermocouple signal at (a) 0T (natural convection) (b) 4T and (c) 9T of magnetic induction for different maximal gradient location $\Delta T = 3$ K and $Ra_T = 1.5 \cdot 10^6$

However the results revealed that addition of paramagnetic particles caused change in the heat transfer nature. Possible explanation of this situation could be that the paramagnetic Cu/CuO nanoparticles acted as mixing agents what caused heat transfer enhancement. What may be concluded that nanofluid should not be treated as one-phase fluid. Moreover, it should be noted that convection changed more in position I, when the magnetic buoyancy forces magnitudes were similar to each other. To understand in detailed the heat transfer processes occurring in the enclosure the convective and conduction heat rates ratios versus magnetic field strength were presented in Figure 4 (b) and (c). The heat rate ratios were calculated as the ratio of actual heat rate to the reference heat rate obtained without magnetic field influence (at natural convection state). The convective heat rates ratios slightly increased with increase of magnetic induction for both experimental enclosure locations. Whereas, the conduction heat rates ratios decreased with magnetic field strength increase for both examined positions. It suggested that conduction was reduced at the expense of convection. The example of one thermocouple signal spectral analysis

is presented in Figure 5. Thermocouple denoted as t6 in Figure 2 was placed inside the experimental enclosure, close to the bottom on the right side. The thermal power spectrum versus the frequency at different maximal gradient location for Cu0.0112 at and $Ra_T = 1.5 \cdot 10^6$ and magnetic induction of 0T (natural convection state), 4 T and 9 T are shown in Figure 5 (a), (b) and (c), respectively. It could be seen that convection for case of maximal gradient located in the middle of enclosure was almost suppressed. Its slight appearance could be found at 9 T (Figure 5 (c)). In Figure 5 (b) the convection was present when maximal gradient was on the top wall, but 9 T of magnetic induction enhanced it.

4 Influence of preparation method

Two-step method of nanofluid preparation involves nanoparticles addition to the base fluid and mixing. Even though, it looks like a simple step, it causes a lot of problems. Therefore there are many publications about proper nanofluids preparation with satisfactorily dispersed particles [9]–[11]. Furthermore, there are no general instruction to prepare all kinds of nanofluids [12]. However the National Institute of Standards and Technology (NIST) and the Center for the Environmental Implications of Nanotechnology (CEINT) published a protocol with some guidelines [13] related to dispersion from powdered nanomaterials with ultrasonic disruption.

The aim of this stage investigation was to verify if the preparation method had an influence on the nanofluid behaviour in the magnetic field. The working fluids were prepared by two different methods, the first one was mechanical agitation for 8 hours, while the second one was ultrasonic homogenization for 30 minutes (with a few pauses preventing fluid overheating) in accordance with [13]. The temperature differences during the thermo-magnetic convection were about 3 K.

The results of Nusselt number dependence on thermo-magnetic Rayleigh number for two kinds of mixing processes (mechanical and ultrasonic agitation) during preparation of Cu0.0112 nanofluid were presented in Figure 6 (a). For mechanically mixed fluid the higher values of Nusselt number could be found. It came from the agglomerates, which were not broken by the mechanical mixing. Therefore, the magnetic buoyancy force had bigger influence on them and in the consequence on the heat transfer processes. To get deeper understanding the convective and conduction heat rates ratios were also calculated and are presented in Figure 6 (b) and (c). The convective heat rates ratios were almost constant for both kinds of preparation methods, however the conduction heat rates ratios slightly increased for the nanofluid being prepared by ultrasonic mixing. At the same time, the conduction heat rates ratio decreased for mechanically mixed nanofluid in higher magnetic fields. The particles uniformly dispersed caused increase in the conducted heat rate. Therefore it could be written that convection was dominated phenomena.

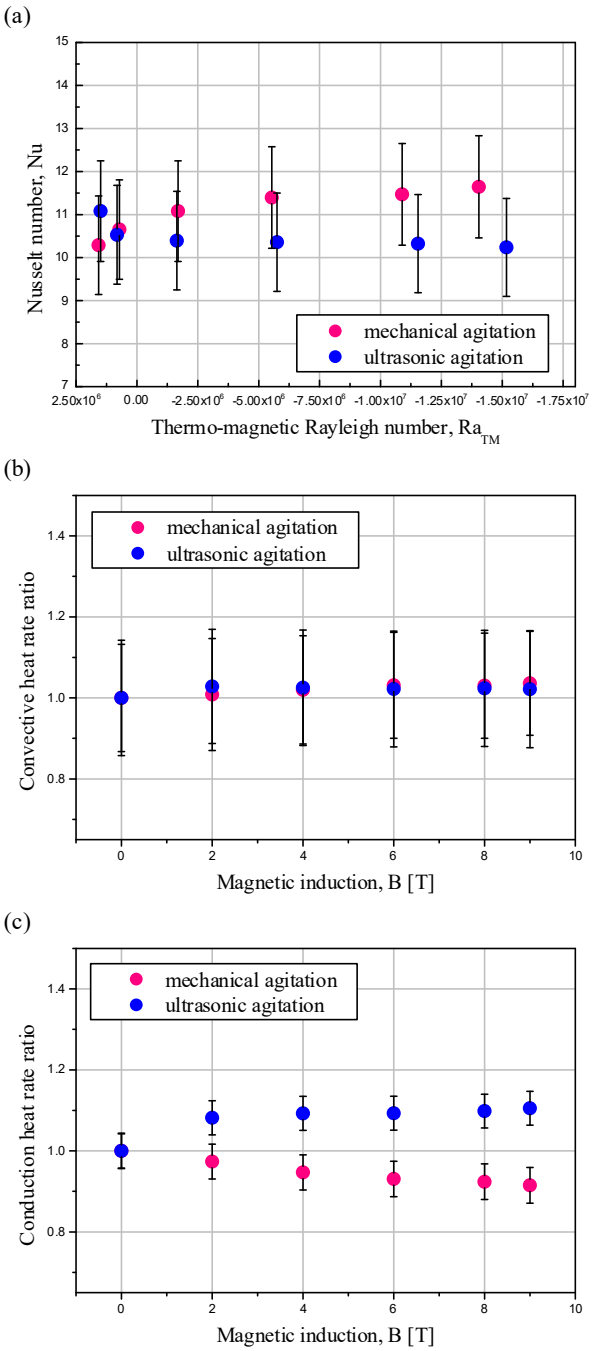

Figure 6. Heat transfer characteristics for various nanofluid preparation methods (a) Nusselt number ratio versus thermo-magnetic Rayleigh number; (b) convective and (c) conduction heat rate ratios versus magnetic induction

The thermal power spectrum versus the frequency at different mixing process for Cu0.0112 and $Ra_T = 1.5 \cdot 10^6$ and magnetic induction of 0T (natural convection state), 4 T and 9 T are shown in Figure 7 (a), (b) and (c), respectively. In Figure 7 (b) two large peaks with low frequency for ultrasonic mixing and a few small ones for mechanical agitation at 4 T were visible, while peaks with small amplitude at 9 T (Figure 7 (c)) were noticed. It could pointed out on big swirls and their reorganization to smaller vortices occurring in the experimental enclosure.

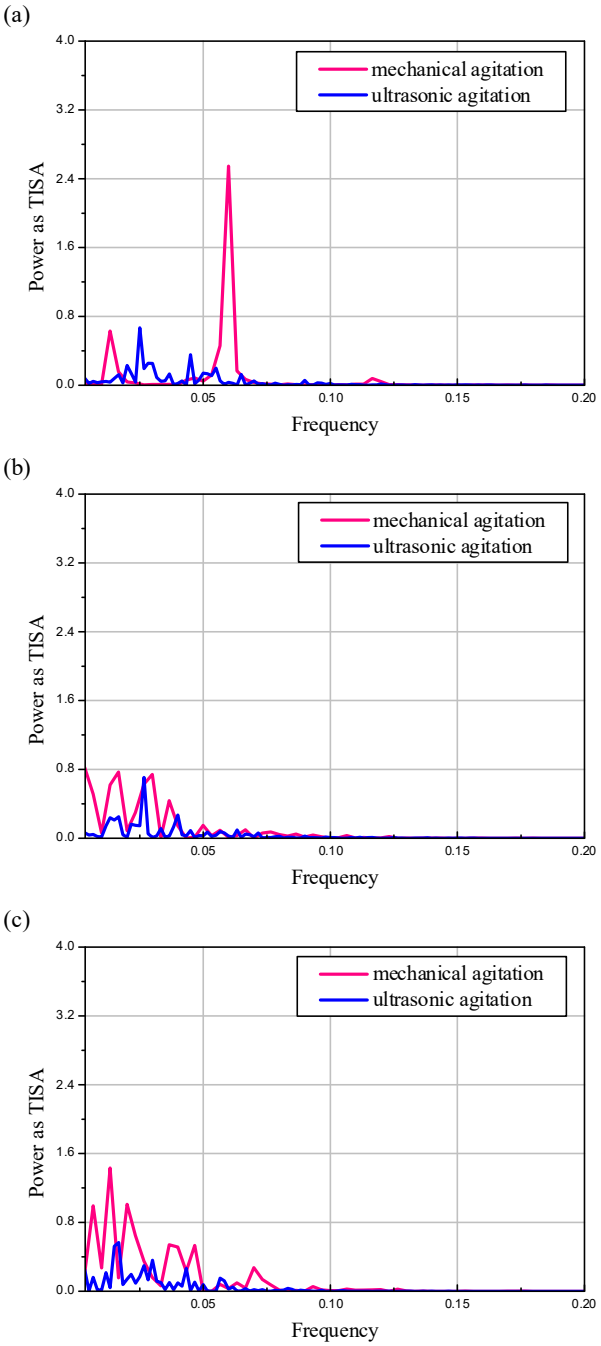

Figure 7. The power spectrum versus frequency for t6 thermocouple signal at (a) 0T (natural convection) (b) 4T and (c) 9T of magnetic induction for the various prepartion method (mechanical and ultrasonic mixing) at ΔT = 3 K and Ra_T = $1.5 \cdot 10^6$

5 Influence of particles concentration

Low concentration nanofluids were examined due to relatively low cost of materials and assumption about electrical non-conductivity. The fluid electrical conductivity level for which it is considered as non-conductive was specified in [14] and equal to 21 S/m. The electrical conductivity of Cu0.112 was 5.518·10-6 S/m (Table 1) [15]. The nanofluids were prepared by two-step method with ultrasonic mixing process and their concentrations were 0.0112, 0.056 and 0.112 vol.%, which

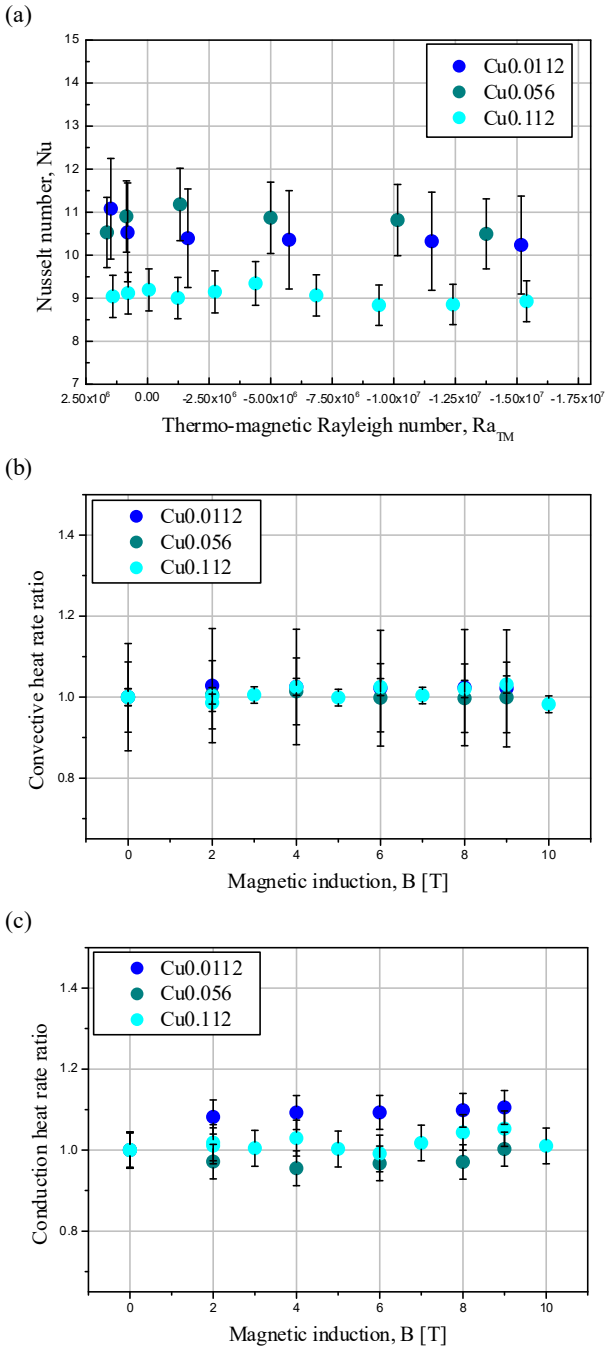

Figure 8. Heat transfer characteristics for various concentrations of nanoparticles (a) Nusselt number versus thermo-magnetic Rayleigh number; (b) convective and (c) conduction heat rate ratios versus magnetic induction

corresponds to abbreviations: Cu0.0112, Cu0.056 and Cu0.112. All properties of working fluids were calculated on the basis of formulas presented in [15] except the magnetic susceptibility which was measured (see Table 1).

The Nusselt number versus thermo-magnetic Rayleigh number for temperature difference of about 3 K for three nanoparticles concentrations at the various magnetic induction values is shown in Figure 8 (a). The Nusselt number decreased with increase of the magnetic field. After an initial increased of the Nusselt number value, it decreased at higher thermo-magnetic Rayleigh number

for all showed cases. The convective heat rate ratio for various magnetic inductions is presented in Figure 8 (b).

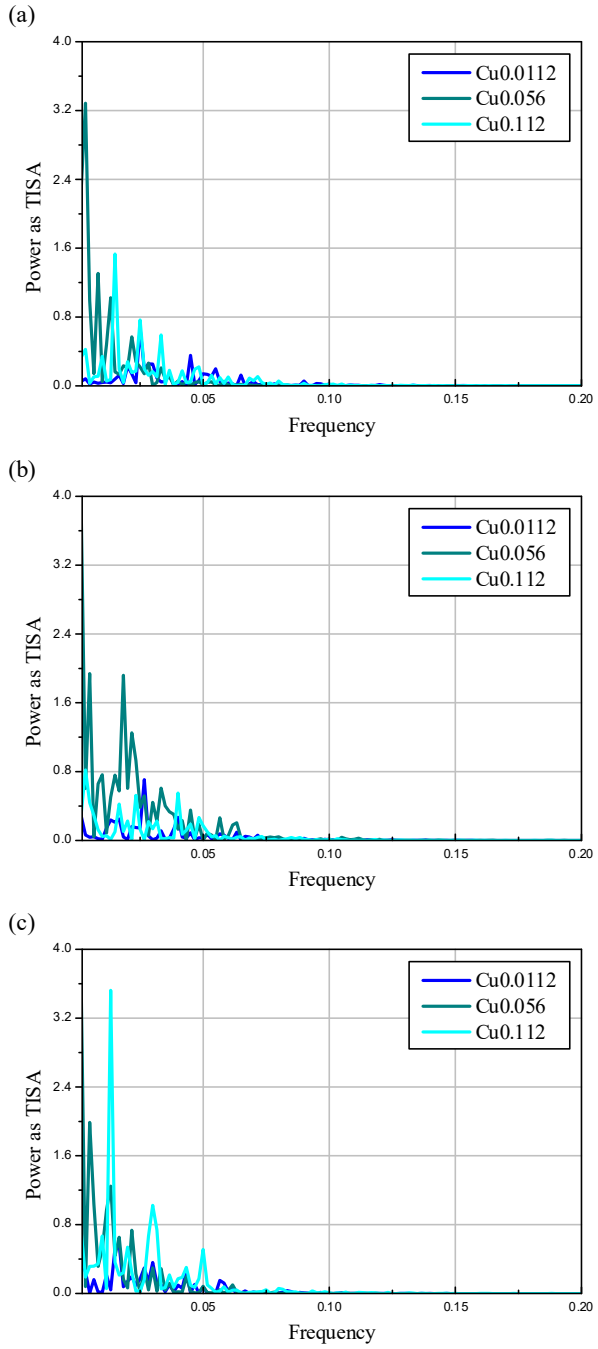

Figure 9. The power spectrum versus frequency for t6 thermocouple signal at (a) 0T (natural convection) (b) 4T and (c) 9T of magnetic induction for the various concentration of copper nanoparticles (ultrasonic mixing process) at $\Delta T = 3$ K and $Ra_T = 1.5 \cdot 10^6$

The ratios remained almost the same for all presented nanofluids concentrations. The conduction heat rate ratio for various magnetic field strength is shown Figure 8 (c). The ratios values are also similar to each other and there is not clear tendency.

Whereas, the thermal power spectra versus the frequencies for various copper nanoparticles concentration at magnetic induction of 0T (natural convection state), 4 T and 9 T are shown in Figure 9 (a), (b) and (c), respectively. For each fluid the peaks changed their frequency and amplitudes. The most important conclusion from the FFT and spectral analysis results is that increasing magnetic induction reorganized flow structure and also energy transported by them, what may have influence on the heat transfer.

6 Discussion and results summary

In this paper the experimental analysis of thermo-magnetic convection of weakly-magnetic, low concentration Cu/CuO nanofluids was presented. The few aspects were taken into account: influence of maximal gradient location, influence of mixing process during nanofluid preparation, influence of Cu/CuO nanoparticles concentration and influence of magnetic induction values. The goal of the paper was accomplished by proven that the magnetic field can enhance heat transfer by low concentration nanofluids. Moreover, it was verified that the nanofluid properties are the main parameters features and taking significant part in these processes.

Interaction of the gravitational and magnetic buoyancy forces, caused by different magnetic properties of the base fluid and nanoparticles, was complex. The theoretical analysis of system forces indicated that there should be convection attenuation observed under applied conditions. However the magnetic buoyancy force acting on the paramagnetic particles led to the heat transfer enhancement. The particles themselves acted as "mixer", which intensified the convection. Therefore, the nanofluid flow cannot be simplified as singe-phase flow in the presented system and under applied conditions.

The results confirmed that the nanofluid preparation is crucial to proper experimental analysis and is strongly related to the nanoparticles size and properties. Moreover, among all of studied parameters the preparation method had the greatest influence on the obtained heat transfer results.

Thermo-magnetic convection of nanofluids with different Cu/CuO nanoparticles concentration showed no clear trend. Therefore, the unequivocal interpretation of this part of presented results cannot be given. This aspect should be thoroughly examined and it will be the next step of the research.

The magnetic field application changed the flow structure what could be observed due to FFT and spectral analysis utilization. The most important conclusion from this research part is that increasing magnetic field reorganized flow structure and therefore, energy transported by the fluid. The experimental analysis will be continued and complemented with the numerical analysis to obtain the description of analysed aspects.

Acknowledgment

The present research was supported by the Polish National Science Centre (Project No. 12/07/B/ST8/03109). The participation in the conference was partially supported by the AGH UST Vice-Rector for Student Affairs, Professor Anna Siwik.

References

1. W. Yu, H. Xie, J. Nanomater. **2012**, 1 (2012)

2. M. T. H. Mosavian, S. Z. Heris, S. Gh. Etemad, M. N. Esfahany, J. Nanoparticle Res. **12**, 7, 2611 (2010)
3. Y. Xuan, Q. Li, Int. J. heat fluid flow **21**, 58 (2000)
4. K. Khanafer, K. Vafai, M. Lightstone, Int. J. Heat Mass Transf. **46**, 9, 3639 (2003)
5. D. Wen, G. Lin, S. Vafaei, K. Zhang, Particuology **7**, 2, 141 (2009)
6. S. U. S. Choi, J. A. Eastman, ASME International Mechanical Engineering Congress & Exposition, (2014)
7. H.Ozoe, S.W.Churchill, AIChE Symp. Ser. Heat Transf. **69**, 126 (1973)
8. A. Roszko, E. Fornalik-Wajs, J. Donizak, J. Wajs, A. Kraszewska, L. Pleskacz, MATEC Web Conf. **6**, 18, 1 (2014)
9. W. Williams, I. Bang, E. Forrest, W. Hu, J. Buonogiorno, Proc. NSTI **2**, 408 (2007)
10. M. Drzazga, Inż. Ap. Chem. **5**, 213 (2012)
11. S. Mukherjee, S. Paria, IOSR J. Mech. Civ. Eng. **9**, 2, 63 (2013)
12. Md. E. Kabir, M. C. Saha, S. Jeelani, Mater. Sci. Eng. A **459**, 1–2, 111 (2007)
13. J. S. Taurozzi, V. A. Hackley, M. R. Wiesner, NIST Spec. Publ. 1200-2 (2012)
14. A. Y. Jianwei Qi, Nobuko I. Wakayama, Int. J. Heat Mass Transf. **44**, 16, 3043 (2001)
15. Y. Xuan, W. Roetzel, Int. J. Heat Mass Transf. **43**, 3701 (2000)